



33 1 Introduction

34 Atmospheric aerosols, also known as particulate matter (PM), are suspensions of
35 fine solid or liquid particles in air. These particles range in diameter from a few
36 nanometers to tens of micrometers. Atmospheric particles contain a variety of non-
37 volatile and semi-volatile compounds including water, sulfates, nitrates, ammonium,
38 dust, trace metals, and organic matter. Many studies have linked increased mortality
39 (Dockery et al., 1993), decreased lung function (Gauderman et al., 2000), bronchitis
40 incidents (Dockery et al., 1996), and respiratory diseases (Pope, 1991; Schwartz et al.,
41 1996; Wang et al., 2008) with elevated PM concentrations. The most readily
42 perceived impact of high particulate matter concentrations is visibility reduction in
43 polluted areas (Seinfeld and Pandis, 2006). Aerosols also play an important role in the
44 energy balance of our planet by scattering and absorbing radiation (Schwartz et al.,
45 1996).

46 Organic aerosol (OA) is a major component of fine PM in most locations
47 around the world. More than 50% of the atmospheric fine aerosol mass is comprised
48 of organic compounds at continental mid-latitudes and as high as 90% in tropical
49 forested areas (Andreae and Crutzen, 1997; Roberts et al., 2001; Kanakidou et al.,
50 2005). Despite their importance, there are many remaining questions regarding their
51 identity, chemistry, lifetime, and in general fate of these organic compounds. OA
52 originates from many different anthropogenic and biogenic sources and processes and
53 has been traditionally categorized into primary OA (POA) which is directly emitted
54 into the atmosphere as particles and secondary OA (SOA) that is formed from the
55 condensation of the oxidation products of volatile (VOCs), intermediate volatility
56 (IVOCs), and semivolatile organic compounds (SVOCs). Both POA and SOA are
57 usually characterized as anthropogenic (aPOA, aSOA) and biogenic (bPOA, bSOA)
58 depending on their sources. In this work we define biomass burning OA (bbOA) as
59 the sum of bbPOA and bbSOA following the terminology proposed by Murphy et al.
60 (2014).

61 Biomass burning is an important global source of air pollutants that affect
62 atmospheric chemistry, climate, and environmental air quality. In this work, the term
63 biomass burning includes wildfires, prescribed burning in forests and other areas,
64 residential wood combustion for heating and other purposes, and agricultural waste
65 burning. Biomass burning is a major source of particulate matter, nitrogen oxides,
66 carbon monoxide, volatile organic compounds, as well as other hazardous air



67 pollutants. Biomass burning contributes around 75% of global combustion POA
68 (Bond et al., 2004). In Europe, biomass combustion is one of the major sources of
69 OA, especially during winter (Puxbaum et al., 2007; Gelencser et al., 2007).

70 Chemical transport models (CTMs) have traditionally treated POA emissions
71 as non-reactive and non-volatile. However, dilution sampler measurements have
72 indicated that POA is clearly semi-volatile (Lipsky and Robinson, 2006; Robinson et
73 al., 2007; Huffman et al., 2009a, 2009b). The semi-volatile character of POA
74 emissions can be described by the volatility basis set (VBS) framework (Donahue et
75 al., 2006; Stanier et al., 2008). The VBS is a scheme of simulating OA accounting for
76 changes in gas-particle partitioning due to dilution, temperature changes, and
77 photochemical aging. The third Fire Lab at Missoula Experiment (FLAME-III)
78 investigated a suite of fuels associated with prescribed burning and wildfires (May et
79 al., 2013). The bbOA partitioning parameters derived from that study are used in this
80 work to simulate the dynamic gas-particle partitioning and photochemical aging of
81 bbOA emissions.

82 A number of modeling efforts have examined the contribution of the semi-
83 volatile bbOA emissions to ambient particulate levels using the VBS framework. For
84 example, Fountoukis et al. (2014) used a three dimensional CTM with an updated
85 wood combustion emission inventory distributing OA emissions using the volatility
86 distribution proposed by Shrivastava et al. (2008). However, this study assumed the
87 same volatility distribution for all OA sources. This volatility distribution is not in
88 general representative of biomass burning emissions since it was derived based on
89 experiments using fossil fuel sources (Shrivastava et al., 2008).

90 The main objective of this study is to develop and test a CTM treating biomass
91 burning organic aerosol (bbOA) emissions separately from all the other anthropogenic
92 and biogenic emissions. This extended model should allow at least in principle more
93 accurate simulation of OA and direct predictions of the role of bbOA in regional air
94 quality. The rest of the manuscript is organized as follows. First, a brief description of
95 the new version of PMCAMx (PMCAMx-SR) is provided. The source-resolved
96 version of PMCAMx (PMCAMx-SR) treats bbOA emissions and their chemical
97 reactions separately from those of other OA sources. The details of the application of
98 PMCAMx-SR in the European domain for a summer and a winter period are
99 presented. In the next section, the predictions of PMCAMx-SR are evaluated using



100 AMS measurements collected in Europe. Finally, the sensitivity of the model to
101 different parameters is quantified.

102

103 **2 PMCAMx-SR description**

104 PMCAMx-SR is a source-resolved version of PMCAMx (Murphy and Pandis,
105 2009; Tsimpidi et al., 2010; Karydis et al., 2010), a three-dimensional chemical
106 transport model that uses the framework of CAMx (Environ, 2003) and simulates the
107 processes of horizontal and vertical advection, horizontal and vertical dispersion, wet
108 and dry deposition, gas, aqueous and aerosol-phase chemistry. The chemical
109 mechanism employed to describe the gas-phase chemistry is based on the SAPRC
110 mechanism (Carter, 2000; Environ, 2003). The version of SAPRC currently used
111 includes 211 reactions of 56 gases and 18 radicals. The SAPRC mechanism has been
112 updated to include gas-phase oxidation of semivolatile organic compounds (SVOCs),
113 intermediate volatility organic compounds (IVOCs). Three detailed aerosol modules
114 are used to simulate aerosol processes: inorganic aerosol growth (Gaydos et al., 2003;
115 Koo et al., 2003), aqueous phase chemistry (Fahey and Pandis, 2001), and secondary
116 organic aerosol (SOA) formation and growth (Koo et al., 2003). The above modules
117 use a sectional approach to dynamically track the size evolution of each aerosol
118 component across 10 size sections spanning the diameter range from 40 nm to 40 μm .

119

120 **2.1 Organic aerosol modelling**

121 PMCAMx-SR simulates organic aerosol based on the volatility basis set (VBS)
122 framework (Donahue et al., 2006; Stanier et al., 2008). VBS is a unified scheme of
123 treating organic aerosol, simulating the volatility, gas-particle partitioning, and
124 photochemical aging of organic pollutant emissions. PMCAMx-SR incorporates
125 separate VBS variables and parameters for the various OA components based on their
126 source.

127

128 **2.1.1 Volatility of primary emissions**

129 PMCAMx-SR assumes that all primary emissions are semi-volatile.
130 According to the VBS scheme, species with similar volatility are lumped into bins
131 expressed in terms of effective saturation concentration values, C^* , separated by
132 factors of 10 at 298 K. POA emissions are distributed across a nine-bin VBS with C^*
133 values ranging from 10^{-2} to $10^6 \mu\text{g m}^{-3}$ at 298 K. SVOCs and IVOCs are distributed



134 among the 1, 10, 100 $\mu\text{g m}^{-3} C^*$ bins and $10^3, 10^4, 10^5, 10^6 \mu\text{g m}^{-3} C^*$ bins
135 respectively. Table 1 lists the generic POA volatility distribution proposed by
136 Shrivastava et al. (2008) assuming that the IVOC emissions are approximately equal
137 to 1.5 times the primary organic aerosol emissions (Robinson et al., 2007; Tsimpidi et
138 al., 2010; Shrivastava et al., 2008). This volatility distribution is used in PMCAMx-
139 SR for all sources with the exception of wood burning. In the original PMCAMx this
140 volatility distribution is also used for wood burning emissions.

141 The partitioning calculations of primary emissions are performed using the
142 same module used to calculate the partitioning of all semi-volatile organic species
143 (Koo et al., 2003). This is based on absorptive partitioning theory and assumes that
144 the bulk gas and particle phases are in equilibrium and that all condensable organics
145 form a pseudo-ideal solution (Odum et al., 1996; Strader et al., 1999). Organic gas-
146 particle partitioning is assumed to depend on temperature and aerosol composition.
147 The Clausius-Clapeyron equation is used to describe the effects of temperature on C^*
148 and partitioning. Table 1 also lists the enthalpies of vaporization currently used in
149 PMCAMx and PMCAMx-SR. All POA species are assumed to have an average
150 molecular weight of 250 g mol^{-1} .

151

152 **2.1.2 Secondary organic aerosol from VOCs**

153 Following Lane et al. (2008a), the SOA VBS-scheme uses four surrogate SOA
154 compounds for each VOC precursor with 4 volatility bins (1, 10, 100, $1000 \mu\text{g m}^{-3}$) at
155 298 K. Anthropogenic (aSOA-v) and biogenic (bSOA-v) components are simulated
156 separately. aSOA components are assumed to have an average molecular weight of
157 150 g mol^{-1} , while bSOA species 180 g mol^{-1} . Laboratory results from the smog-
158 chamber experiments of Ng et al. (2006) and Hildebrandt et al. (2009) are used for the
159 anthropogenic aerosol yields.

160

161 **2.1.3 Chemical aging mechanism**

162 All OA components are treated as chemically reactive in PMCAMx-SR.
163 Vapors resulting from the evaporation of POA are assumed to react with OH radicals
164 with a rate constant of $k = 4 \times 10^{-11} \text{ cm}^3 \text{ molec}^{-1} \text{ s}^{-1}$ resulting in the formation of
165 oxidized OA. These reactions are assumed to lead to an effective reduction of
166 volatility by one order of magnitude. Semi-volatile SOA components are also
167 assumed to react with OH in the gas phase with a rate constant of $k = 1 \times 10^{-11} \text{ cm}^3$



168 molec⁻¹ s⁻¹ for anthropogenic SOA (Atkinson and Arey, 2003). Biogenic SOA aging
169 is assumed to lead to zero net change of volatility (Lane et al., 2008b). Each reaction
170 is assumed to increase the OA mass by 7.5% to account for added oxygen.
171

172 2.2 PMCAMx-SR enhancements

173 In PMCAMx-SR, the fresh biomass burning organic aerosol (bbOA) and its
174 secondary oxidation products (bbSOA) are simulated separately from the other POA
175 components. The May et al. (2013) volatility distribution is used to simulate the gas-
176 particle partitioning of fresh bbOA. This distribution includes surrogate compounds
177 up to a volatility of 10⁴ µg m⁻³. This means that the more volatile IVOCs, which could
178 contribute to SOA formation, are not included. To close this gap, the values of the
179 volatility distribution of Robinson et al. (2007) are used for the 10⁵ and 10⁶ µg m⁻³
180 bins (Table 1). The sensitivity of PMCAMx-SR to the IVOC emissions added to the
181 May et al. (2013) distribution will be explored in a subsequent section. The effective
182 saturation concentrations and the enthalpies of vaporization used for bbOA in
183 PMCAMx-SR are also listed in Table 1. The new bbOA scheme requires the
184 introduction of 36 new organic species to simulate both phases of fresh primary and
185 oxidized bbOA components. The rate constant used for the chemical aging reactions
186 is the same as the one currently used for all POA components and has a value of $k = 4$
187 $\times 10^{-11}$ cm³ molec⁻¹ s⁻¹. The volatility distributions of bbOA in PMCAMx and
188 PMCAMx-SR are shown in Fig. 1a. The volatility distribution implemented in
189 PMCAMx-SR results in less volatile bbOA for ambient OA levels (a few µg m⁻³)
190 (Fig. 1b).

191

192 3 Model application

193 PMCAMx-SR was applied to a 5400×5832 km² region covering Europe with
194 36×36 km grid resolution and 14 vertical layers extending up to 6 km. The model was
195 set to perform simulations on a rotated polar stereographic map projection. The
196 necessary inputs to the model include horizontal wind components, temperature,
197 pressure, water vapor, vertical diffusivity, clouds, and rainfall. All meteorological
198 inputs were created using the meteorological model WRF (Weather Research and
199 Forecasting) (Skamarock et al., 2005). The simulations were performed during a



200 summer (1-29 May 2008) and a winter period (25 February-22 March 2009). In order
201 to limit the effect of the initial conditions on the results, the first two days of each
202 simulation were excluded from the analysis.

203 Anthropogenic and biogenic emissions in the form of hourly gridded fields
204 were developed both for gases and primary particulate matter. Anthropogenic gas
205 emissions include land emissions from the GEMS dataset (Visschedijk et al., 2007)
206 and also emissions from international shipping activities. Anthropogenic particulate
207 matter mass emissions of organic and elemental carbon are based on the Pan-
208 European Carbonaceous Aerosol Inventory (Denier van der Gon et al., 2010) that has
209 been developed as part of the EUCAARI project activities (Kulmala et al., 2009). All
210 relevant significant emission sources are included in the two inventories. Emissions
211 from ecosystems were calculated offline by MEGAN (Model of Emissions of Gases
212 and Aerosols from Nature) (Guenther et al., 2006). The marine aerosol emission
213 model developed by O'Dowd et al. (2008) has been used to estimate mass fluxes for
214 both accumulation and coarse mode including the organic aerosol fraction. Wind
215 speed data from WRF and chlorophyll-a concentrations are the inputs needed for the
216 marine aerosol emissions module.

217 Day-specific wildfire emissions were also included (Sofiev et al., 2008a; 2008b).
218 Anthropogenic sources of wood combustion include residential heating and
219 agricultural activities. The gridded emission inventories of bbOA species for the two
220 modeled periods are shown in Fig. 2. During the early summer simulated period
221 wildfires were responsible for 60% of the bbOA emissions, agricultural waste burning
222 for 15% and residential wood combustion for 25% (Table 2). Details about the OA
223 emission rates from agricultural activities are provided in the Supplementary
224 Information (Fig. S1). During winter residential combustion is the dominant source
225 (63%). The wintertime wildfire emissions in the inventory, approximately 3,000 tn
226 d⁻¹, are quite high especially when compared with the corresponding summer value
227 which is 1,700 tn d⁻¹. The spatial distribution of OA emission rates from wildfires
228 during 25 February-22 March 2009 is provided in the Supplementary Information
229 (Fig. S2). Analysis of fire counts in satellite observations used for the development of
230 the inventory suggests that some agricultural emissions have probably been attributed
231 to wildfires. All bbOA sources are treated the same way in PMCAMx-SR so this
232 potential misattribution does not affect our results.

233



234 **4 PMCAMx-SR testing**

235 To test our implementation of the source-resolved VBS in PMCAMx-SR we
236 compared its results with those of PMCAMx using the same VBS parameters. For this
237 test we used in PMCAMx-SR the default PMCAMx bbOA partitioning parameters
238 shown in Table 1 as proposed by Shrivastava et al. (2008). In this way both models
239 should simulate the bbOA in exactly the same way, but PMCAMx-SR describes it
240 independently while PMCAMx lumps it with other primary OA. The differences
241 between the corresponding OA concentrations predicted by the two models were on
242 average less than $10^{-3} \mu\text{g m}^{-3}$ (0.03%). The maximum difference was approximately
243 $0.03 \mu\text{g m}^{-3}$ (0.6%) in western Germany. This suggests that our changes to the code of
244 PMCAMx to develop PMCAMx-SR did not introduce any inconsistencies with the
245 original model. The small differences are due to numerical issues in the
246 advection/dispersion calculations.

247

248 **5 Contribution of bbOA to PM over Europe**

249 In this section the predictions of PMCAMx-SR for the base case simulations
250 during 1 - 29 May 2008 and 25 February - 22 March 2009 are analysed. Figure 3
251 shows the PMCAMx-SR predicted average ground-level $\text{PM}_{2.5}$ concentrations for the
252 various OA components for the two simulated periods.

253 The POA from non-bbOA sources will be called fossil POA (fPOA) in the rest
254 of the paper. fPOA levels over Europe were on average around $0.1 \mu\text{g m}^{-3}$ during both
255 periods (Figs. 3a and 3b). However, their spatial distributions are quite different.
256 During May, predicted fPOA concentrations are as high as $2 \mu\text{g m}^{-3}$ in polluted areas
257 in central and northern Europe but are less than $0.5 \mu\text{g m}^{-3}$ in the rest of the domain.
258 These low levels are due to the evaporation of POA in this warm period. For the
259 winter period peak fPOA levels are higher reaching values of around $3.5 \mu\text{g m}^{-3}$ in
260 Paris and Moscow. fPOA contributes approximately 3.5% and 6% to total OA in
261 Europe during May 2008 and February-March 2009 respectively. bbPOA
262 concentrations have peak average values $7 \mu\text{g m}^{-3}$ in St. Petersburg in Russia and 10
263 $\mu\text{g m}^{-3}$ in Porto in Portugal during summer and winter respectively (Figures 3c and
264 3d). During the summer bbPOA is predicted to contribute 5% to total OA, and its
265 contribution during winter increases to 32%. The average predicted bbOA
266 concentrations over Europe are $0.1 \mu\text{g m}^{-3}$ and $0.8 \mu\text{g m}^{-3}$ during the summer and the
267 winter period respectively.



268 The SOA resulting from the oxidation of IVOCs (SOA-iv) and evaporated
269 POA (SOA-sv) has concentrations as high as $1 \mu\text{g m}^{-3}$ in central Europe and the
270 average levels are around $0.3 \mu\text{g m}^{-3}$ (13% contribution to total OA) during summer
271 (Fig. 3e). During winter the peak concentration value was a little less than $0.5 \mu\text{g m}^{-3}$
272 in Moscow in Russia and the average levels were approximately $0.1 \mu\text{g m}^{-3}$ (5.5%
273 contribution to total OA) (Fig 3f). The highest average concentration of bbSOA-sv
274 and bbSOA-iv (biomass burning SOA from intermediate volatility and semi-volatile
275 precursors) was approximately $1 \mu\text{g m}^{-3}$ in Lecce in Italy during summer and $3.5 \mu\text{g m}^{-3}$
276 in Porto during winter. During May bbSOA is predicted to contribute 11% to total
277 OA over Europe and during February-March 2009 its predicted contribution is 15%.
278 The average bbSOA is $0.3 \mu\text{g m}^{-3}$ during summer and approximately $0.4 \mu\text{g m}^{-3}$
279 during winter (Figs. 3g and 3h). During the summer, the remaining 67% of total OA is
280 biogenic SOA (52%) and anthropogenic SOA (15%), and in winter of the remaining
281 41% of total OA, 36% is biogenic and 5% is anthropogenic SOA (not shown).

282 In areas like St. Petersburg in Russia predicted hourly bbOA levels exceeded
283 $300 \mu\text{g m}^{-3}$ due to the nearby fires affecting the site on May 3-5 (Fig. 4). For these
284 extremely high concentrations most of the bbOA (90% for St. Petersburg) was
285 primary with the bbSOA contributing around 10%. The spatiotemporal evolution of
286 bbPOA and bbSOA during May 1–6 in Scandinavia and northwest Russia is depicted
287 in Figure 5. A series of fires started in Russia on May 1, becoming more intense
288 during the next days until May 6 when they were mostly extinguished. bbSOA, as
289 expected, follows the opposite evolution with low concentration values in the
290 beginning of the fire events (May 1) and higher values later on. The bbSOA
291 production increases the range of influence of the fires.

292 In Majden (FYROM) fires contributed up to $25 \mu\text{g m}^{-3}$ of bbOA on May 25-
293 26. The bbSOA was 15% of the bbOA in this case (Fig. S3). Fires also occurred in
294 south Italy (Catania) and contributed up to $52 \mu\text{g m}^{-3}$ of OA on May 15-17. During
295 this period the bbSOA was 13% of the bbOA (Fig. S3). Paris (France) and Dusseldorf
296 (Germany) were further away from major fires but were also affected by fire
297 emissions during most of the month (Fig. S3). The maximum hourly bbOA levels in
298 these cities were around $5 \mu\text{g m}^{-3}$, but bbSOA in this case represents according to the
299 model around 35% of the total bbOA in Paris and 55% in Dusseldorf.

300 During the winter simulation period, there were major fires during March 20-
301 22 in Portugal and northwestern Spain. The maximum predicted hourly bbOA



302 concentration in Porto (Portugal) exceeded $700 \mu\text{g m}^{-3}$ on March 21. During the same
303 3 days in March the average levels of bbPOA in Portugal and Spain were $9 \mu\text{g m}^{-3}$
304 and their contribution to total OA was 62%. bbPOA was 80% of the total bbOA
305 during March 20-22 in the Iberian Peninsula.

306

307 **6 Role of the more volatile IVOCs**

308 We performed an additional sensitivity simulation where we assumed that there
309 are no emissions of more volatile IVOCs (those in the 10^5 and $10^6 \mu\text{g m}^{-3}$ bins). The
310 partitioning parameters used in this sensitivity test are shown in Table 1. The
311 emissions rates for each volatility bin during the two modeled periods are provided in
312 the Supplementary Information (Table S1). The absolute emissions assigned to the
313 lower volatility bins are approximately the same for both simulations. More
314 specifically, during May 2008, the emission rates of LVOCs (10^{-2} , $10^{-1} \mu\text{g m}^{-3} \text{C}^*$
315 bins) and SVOCs (10^0 , 10^1 , $10^2 \mu\text{g m}^{-3} \text{C}^*$ bins) are 530 and 1050 tn d^{-1} respectively
316 for the base-case run and 580 and 1160 tn d^{-1} respectively for the sensitivity run.
317 During February-March 2009, the emission rates of LVOCs and SVOCs are 2100 and
318 4100 tn d^{-1} respectively for the base-case run and 2300 and 4500 tn d^{-1} respectively
319 for the sensitivity run. The base case simulation assumes higher emissions in the
320 upper volatility bins of the IVOCs (10^3 , 10^4 , 10^5 , $10^6 \mu\text{g m}^{-3} \text{C}^*$ bins) which can be
321 converted to bbSOA. During summer, the emission rate of IVOCs is 4460 tn d^{-1} in the
322 base-case run and 1160 tn d^{-1} in the sensitivity test. During winter, the emission rate
323 of IVOCs is 17400 tn d^{-1} in the base case and 4500 tn d^{-1} in the sensitivity test.

324 The base case and the sensitivity simulations predict practically the same
325 bbPOA concentrations in both periods (Fig. 6) as expected based on the emission
326 inventory. During summer, the average absolute change of bbPOA in Europe is
327 around 10% (corresponding to $0.01 \mu\text{g m}^{-3}$) (Fig. 6a). The average difference in
328 bbSOA is significantly higher and around 60% ($0.2 \mu\text{g m}^{-3}$ on average) due to the
329 higher IVOC emissions of the base case simulation. The atmospheric conditions
330 during this warm summer period (high temperature, UV radiation, relative humidity)
331 lead to high OH concentrations and rapid production of bbSOA.

332 During winter, the average absolute change for both bbPOA and bbSOA in
333 Europe is approximately $0.1 \mu\text{g m}^{-3}$ (Fig. 6b and 6f). These correspond to 15% change
334 for the primary and 25% for the secondary bbOA levels. The maximum difference for
335 average bbPOA is approximately $5 \mu\text{g m}^{-3}$ and for bbSOA around $1.5 \mu\text{g m}^{-3}$ both in



336 northwestern Portugal. However, during the fire period (March 20-22) in Spain and
337 Portugal the maximum concentration difference between the two cases was $20 \mu\text{g m}^{-3}$
338 for bbPOA and $7 \mu\text{g m}^{-3}$ for bbSOA.

339 Figure 7 shows the total bbOA (sum of bbPOA and bbSOA) during both
340 periods. Higher bbOA concentrations are predicted in the base case simulation due to
341 the higher bbSOA concentrations from higher IVOC emissions. During summer the
342 contributions of the biomass burning IVOC oxidation products to total bbOA exceed
343 30% over most of Europe, while during winter these components are important
344 mostly over Southern Europe and the Mediterranean (Fig. S4).

345

346 7 Comparison with field measurements

347 In order to assess the PMCAMx-SR performance during the two simulation
348 periods the model's predictions were compared with AMS hourly measurements that
349 took place in several sites around Europe. All observation sites are representative of
350 regional atmospheric conditions.

351 The PMF technique (Paatero and Tapper, 1994; Lanz et al., 2007; Ulbrich et
352 al., 2009; Ng et al., 2010) was used to analyze the AMS organic spectra providing
353 information about the sources contributing to the OA levels (Hildebrandt et al., 2010;
354 Morgan et al., 2010). The method classifies OA into different types based on different
355 temporal emission and formation patterns and separates it into hydrocarbon-like
356 organic aerosol (HOA, a POA surrogate), oxidized organic aerosol (OOA, a SOA
357 surrogate) and fresh bbOA. Additionally, factor analysis can further classify OOA
358 into more and less oxygenated OOA components. Fresh bbOA can be compared
359 directly to the PMCAMx-SR bbPOA predictions, whereas bbSOA should, in principle
360 at least, be included in the OOA factors. The AMS HOA can be compared with
361 predicted fresh POA. The oxygenated AMS OA component can be compared against
362 the sum of anthropogenic and biogenic SOA (aSOA, bSOA), SOA-sv and SOA-iv,
363 bbSOA and OA from long range transport.

364 PMCAMx-SR performance is quantified by calculating the mean bias (MB),
365 the mean absolute gross error (MAGE), the fractional bias (FBIAS), and the fractional
366 error (FERROR) defined as:

$$367 \quad \text{MB} = \frac{1}{n} \sum_{i=1}^n (P_i - O_i) \quad \text{MAGE} = \frac{1}{n} \sum_{i=1}^n |P_i - O_i|$$



$$\text{FBIAS} = \frac{2}{n} \sum_{i=1}^n \frac{P_i - O_i}{P_i + O_i} \quad \text{FERROR} = \frac{2}{n} \sum_{i=1}^n \frac{|P_i - O_i|}{P_i + O_i}$$

368

369 where P_i is the predicted value of the pollutant concentration, O_i is the observed value
370 and n is the number of measurements used for the comparison. AMS measurements
371 are available in 4 stations (Cabauw, Finokalia, Melpitz and Mace Head) during 1-29
372 May 2008 and 7 stations (Cabauw, Helsinki, Mace Head, Melpitz, Hyttiala, Barcelona and
373 Chilbolton) during 25 February-23 March 2009.

374

375 During May 2008 a bbPOA factor was identified based on the PMF analysis
376 of the measurements only in Cabauw and Mace Head. In the other two sites
377 (Finokalia and Melpitz) PMCAMx-SR predicted very low average bbPOA levels (less
378 than $0.1 \mu\text{g m}^{-3}$), so its predictions for these sites can be viewed as consistent with the
379 results of the PMF analysis. Figure 8 shows the comparison of the predicted bbPOA
380 by PMCAMx-SR with the observed values in Cabauw. The average AMS-PMF bbOA
381 was $0.4 \mu\text{g m}^{-3}$ and the predicted average bbPOA by PMCAMx-SR was also $0.4 \mu\text{g m}^{-3}$.
382 The mean bias was only $-0.01 \mu\text{g m}^{-3}$. The model however tended to overpredict
383 during the first 10 days and to underpredict during the last week. In Mace Head
384 PMCAMx-SR predicts high bbOA levels during May 14 – 15, but unfortunately the
385 available measurements started on May 16. During the last two weeks of the
386 simulation the model predicts much lower bbOA levels (approximately $0.35 \mu\text{g m}^{-3}$
387 less) than the AMS-PMF analysis. The same problem was observed in Cabauw
388 suggesting potential problems with the fire emissions during this period.

388

389 During winter the model tends to overpredict the observed bbOA values in
390 Barcelona, Cabauw, Melpitz, Helsinki and Hyttiala. On the other hand, the model
391 underpredicts the bbOA in Mace Head and Chilbolton by approximately $0.3 \mu\text{g m}^{-3}$
392 on average. The prediction skill metrics of PMCAMx-SR (base case and sensitivity test)
393 against AMS factor analysis during the modelled periods are also provided in the
394 Supplementary Information (Tables S2-S5). These problems in reproducing
395 wintertime OA measurements were also noticed by Denier van der Gon et al. (2015)
396 and suggest problems in the emissions and/or the simulation of the bbOA during this
397 cold period with slow photochemistry.

397

398 8 Conclusions

399 A source-resolved version of PMCAMx, called PMCAMx-SR was developed and
400 tested. This new version can be used to study independently specific organic aerosol



401 sources (eg. diesel emissions) if so desired by the user. We applied PMCAMx-SR to
402 the European domain during an early summer and a winter period focusing on
403 biomass burning.

404 The concentrations of bbOA (sum of bbPOA and bbSOA) and their
405 contributions to total OA over Europe are, as expected, quite variable in space and
406 time. During the early summer, the contribution of bbOA to total OA over Europe
407 was predicted to be 16%, while during winter it increased to 47%. Secondary biomass
408 burning OA was predicted to be approximately 70% of the bbOA during summer and
409 only 30% during the winter on average. The production of bbSOA increases the range
410 of influence of fires.

411 The IVOCs emitted by the fires can be a major source of SOA. In our
412 simulations, the IVOCs with saturation concentrations $C^*=10^5$ and $10^6 \mu\text{g m}^{-3}$
413 contributed approximately one third of the average bbOA over Europe. The emissions
414 of these compounds and their aerosol forming potential are uncertain, so the
415 formation of bbSOA clearly is an importance topic for future work.

416 PMCAMx-SR was evaluated against AMS measurements taken at various
417 European measurement stations and the results of the corresponding PMF analysis.
418 During the summer the model reproduced without bias the average measured bbPOA
419 levels in Cabauw and the practically zero levels in Finokalia and Melpitz. However, it
420 underpredicted the bbPOA in Mace Head. Its performance for oxygenated organic
421 aerosol (OOA) which should include bbSOA together with a lot of other sources was
422 mixed: overprediction in Cabauw (fractional bias +42%), Mace Head (fractional bias
423 +34%), and Finokalia (fractional bias +23%) and underprediction in Melpitz
424 (fractional bias -14%).

425 During the winter the model overpredicted the bbPOA levels in most stations
426 (Cabauw, Helsinki, Melpitz, Hyytiala, Barcelona), while it underpredicted in Mace
427 Head and Chibolton. At the same time, it reproduced the measured OOA
428 concentrations with less than 15% bias in Cabauw, Helsinki, and Hyytiala,
429 underpredicted OOA in Melpitz, Barcelona, and Chibolton and overpredicted OOA in
430 Mace Head. These results both potential problems with the wintertime emissions of
431 bbPOA and the production of secondary OA during the winter.



432 *Data availability.* The data in the study are available from the authors upon request
433 (spyros@chemeng.upatras.gr).

434

435 *Author contributions.* GNT conducted the simulations, analysed the results, and wrote
436 the paper. SNP was responsible for the design of the study, the synthesis of the results
437 and contributed to the writing of the paper.

438 *Competing interests.* The authors declare that they have no conflict of interest.

439 *Acknowledgements.* This study was financially supported by the European Union's
440 Horizon 2020 EUROCHAMP-2020 Infrastructure Activity (Grant agreement 730997)
441 and the Western Regional Air Partnership (WRAP Project No. 178-14).

442

443 **References**

- 444 Aiken, A. C., Salcedo, D., Cubison, M. J., Huffman, J. A., DeCarlo, P. F., Ulbrich, I.
445 M., Docherty, K. S., Sueper, D., Kimmel, J. R., Worsnop, D. R., Trimborn, A.,
446 Northway, M., Stone, E. A., Schauer, J. J., Volkamer, R. M., Fortner, E., de
447 Foy, B., Wang, J., Laskin, A., Shutthanandan, V., Zheng, J., Zhang, R.,
448 Gaffney, J., Marley, N. A., Paredes-Miranda, G., Arnott, W. P., Molina, L. T.,
449 Sosa, G., and Jimenez, J. L.: Mexico City aerosol analysis during MILAGRO
450 using high resolution aerosol mass spectrometry at the urban supersite (T0) -
451 Part 1: Fine particle composition and organic source apportionment, Atmos.
452 Chem. Phys., 9, 6633–6653, doi:10.5194/acp-9-6633-2009, 2009.
- 453 Allan, J. D., Alfarra, M. R., Bower, K. N., Williams, P. I., Gallagher, M. W., Jimenez,
454 J. L., McDonald, A. G., Nemitz, E., Canagaratna, M. R., Jayne, J. T., Coe, H.,
455 and Worsnop, D. R.: Quantitative sampling using an Aerodyne Aerosol Mass
456 Spectrometer, Part 2: Measurements of fine particulate chemical composition
457 in two UK Cities, J. Geophys. Res., 108, 4091, doi:4010.1029/2002JD002359,
458 2003.
- 459 Andreae, M. O. and Crutzen, P. J.: Atmospheric aerosols: biogeochemical sources and
460 role in atmospheric chemistry. Science, 276, 1052–1058, 1997.
- 461 Bond, T.C., Streets, D.G., Yarber, K.F., Nelson, S.M., Woo, J.H., and Klimont, Z.: A
462 technology-based global inventory of black and organic carbon emissions
463 from combustion, J. Geophys. Res., 109, doi:10.1029/2003JD003697, 2004.
- 464 Burtraw, D., Krupnick, A., Mansur, E., Austin, D., and Farrell, D.: Costs and benefits
465 of reducing air pollutants related to acid rain, Contemp. Econ. Policy, 16, 379–
466 400, 2007.
- 467 Carter, W.P.L.: Programs and files implementing the SAPRC-99 mechanism and its
468 associated emissions processing procedures for Models-3 and other regional
469 models, www.cert.ucr.edu/~carter/SAPRC99/, 2000.
- 470 Crippa, M., Canonaco, F., Lanz, V. A., Äijälä, M., Allan, J. D., Carbone, S., Capes,
471 G., Dall'Osto, M., Day, D. A., DeCarlo, P. F., Di Marco, C. F., Ehn, M.,
472 Eriksson, A., Freney, E., Hildebrandt Ruiz, L., Hillamo, R., Jimenez, J.-L.,



- 473 Junninen, H., Kiendler-Scharr, A., Kortelainen, A.-M., Kulmala, M., Mensah,
474 A. A., Mohr, C., Nemitz, E., O'Dowd, C., Ovadnevaite, J., Pandis, S. N.,
475 Petäjä, T., Poulain, L., Saarikoski, S., Sellegri, K., Swietlicki, E., Tiitta, P.,
476 Worsnop, D. R., Baltensperger, U., and Prévôt, A. S. H.: Organic aerosol
477 components derived from 25 AMS data sets across Europe using a consistent
478 ME-2 based source apportionment approach, *Atmos. Chem. Phys.*, 14, 6159-
479 6176, 2014.
- 480 Cubison, M. J., Ortega, A. M., Hayes, P. L., Farmer, D. K., Day, D., Lechner, M. J.,
481 Brune, W. H., Apel, E., Diskin, G. S., Fisher, J. A., Fuelberg, H. E., Hecobian,
482 A., Knapp, D. J., Mikoviny, T., Riemer, D., Sachse, G. W., Sessions, W.,
483 Weber, R. J., Weinheimer, A. J., Wisthaler, A., and Jimenez, J. L.: Effects of
484 aging on organic aerosol from open biomass burning smoke in aircraft and
485 laboratory studies, *Atmos. Chem. Phys.*, 11, 12049–12064, 2011.
- 486 Denier van der Gon, H. A. C., Visschedijk, A., van der Brugh, H., and Droge, R.: A
487 high resolution European emission data base for the year 2005, TNO report
488 TNO-034-UT-2010-01895 RPTML, Utrecht, the Netherlands, 2010.
- 489 Denier van der Gon, H.A.C., Visschedijk, A., Fountoukis, C., Pandis, S.N.,
490 Bergstrom, R., Simpson, D., and Johansson, C.: Particulate emissions from
491 residential wood combustion in Europe - Revised estimates and an evaluation,
492 *Atmos. Chem. Phys.*, 15, 6503-6519, 2015.
- 493 Dockery, W. D., C. A. Pope, X. Xu, J. D. Spengler, J. H. Ware, M. E. Fay, Jr., B. G.
494 Ferris, F. E., and Speizer: An association between air pollution and mortality
495 in six U.S. cities, *The New England Journal of Medicine*, 329, 1753-1759,
496 1993.
- 497 Dockery, D. W., Cunningham J., Damokosh A. I., Neas L. M., Spengler J. D.,
498 Koutrakis P., Ware J. H., Raizenne M., and Speizer F. E.: Health effects of
499 acid aerosols on North America children: Respiratory symptoms,
500 *Environmental Health Perspectives*, 104, 26821-26832, 1996.
- 501 Donahue, N. M., Robinson, A. L., Stanier, C. O., and Pandis, S. N.: Coupled
502 partitioning, dilution, and chemical aging of semivolatile organics, *Environ.*
503 *Sci. Technol.*, 40, 2635–2643, 2006.
- 504 EFFIS (European Forest Fire Information System (EFFIS)) Available at:
505 <http://effis.jrc.ec.europa.eu/>.
- 506 ENVIRON: User's Guide to the Comprehensive Air Quality Model with Extensions
507 (CAMx), Version 4.02, Report, ENVIRON Int. Corp., Novato, Calif.,
508 available at: <http://www.camx.com>, 2003.
- 509 Fahey, K. and Pandis, S. N.: Optimizing model performance: variable size resolution
510 in cloud chemistry modelling, *Atmos. Environ.*, 35, 4471–4478, 2001.
- 511 Fountoukis, C., Racherla, P. N., Denier van der Gon, H. A. C., Polymeneas, P.,
512 Charalampidis, P. E., Pilinis, C., Wiedensohler, A., Dall'Osto, M., O'Dowd,
513 C., and Pandis, S. N.: Evaluation of a three-dimensional chemical transport
514 model (PMCAMx) in the European domain during the EUCAARI May 2008
515 campaign, *Atmos. Chem. Phys.*, 11, 10331–10347, 2011.
- 516 Fountoukis, C., Butler, T., Lawrence, M. G., Denier van der Gon, H. A. C.,
517 Visschedijk, A. J. H., Charalampidis, P., Pilinis, C., and Pandis, S. N.: Impacts
518 of controlling biomass burning emissions on wintertime carbonaceous aerosol
519 in Europe, *Atmos. Environ.*, 87, 175–182, 2014.
- 520 Gauderman, W. J., McConnel R., Gilliland F., London S., Thomas D., Avol E., Vora
521 H., Berhane K., Rappaport E. B., Lurmann F., Margolis H. G., and Peters J.:
522 Association between air pollution and lung function growth in southern



- 523 California children, *American Journal of Respiratory and Critical Care*
524 *Medicine*, 162, 1383-1390, 2000.
- 525 Gaydos, T., Koo, B., and Pandis, S. N.: Development and application of an efficient
526 moving sectional approach for the solution of the atmospheric aerosol
527 condensation/evaporation equations, *Atmos. Environ.*, 37, 3303–3316, 2003.
- 528 Gelencser, A., May, B., Simpson, D., Sanchez-Ochoa, A., Kasper-Giebl, A.,
529 Puxbaum, H., Caseiro, A., Pio, C., and Legrand, M.: Source apportionment of
530 PM_{2.5} organic aerosol over Europe: primary/secondary, natural/
531 anthropogenic, fossil/biogenic origin, *J. Geophys. Res.* 112, D23S04,
532 doi:10.1029/2006JD008094, 2007.
- 533 Guenther, A., Karl, T., Harley, P., Wiedinmyer, C., Palmer, P. I., and Geron, C.:
534 Estimates of global terrestrial isoprene emissions using MEGAN (Model of
535 Emissions of Gases and Aerosols from Nature), *Atmos. Chem. Phys.*, 6, 3181–
536 3210, 2006.
- 537 Hennigan, C. J., Sullivan, A. P., Collett, J. L., and Robinson, A. L.: Levoglucosan
538 stability in biomass burning particles exposed to hydroxyl radicals, *Geophys.*
539 *Res. Lett.*, 37, L09806, doi:10.1029/2010GL043088, 2010.
- 540 Hennigan, C. J., Miracolo, M. A., Engelhart, G. J., May, A. A., Presto, A. A., Lee, T.,
541 Sullivan, A. P., McMeeking, G. R., Coe, H., Wold, C. E., Hao, W.-M.,
542 Gilman, J. B., Kuster, W. C., de Gouw, J., Schichtel, B. A., J. L. Collett Jr.,
543 Kreidenweis, S. M., and Robinson, A. L.: Chemical and physical
544 transformations of organic aerosol from the photo-oxidation of open biomass
545 burning emissions in an environmental chamber, *Atmos. Chem. Phys.*, 11,
546 7669–7686, 2011.
- 547 Hildebrandt, L., Donahue, N. M., and Pandis, S. N.: 2009. High formation of
548 secondary organic aerosol from the photo-oxidation of toluene, *Atmos. Chem.*
549 *Phys.*, 9, 2973–2986.
- 550 Hildebrandt, L., Engelhart, G. J., Mohr, C., Kostenidou, E., Lanz, V. A., Bougiatioti,
551 A., DeCarlo, P. F., Prevot, A. S. H., Baltensperger, U., Mihalopoulos, N.,
552 Donahue, N. M., and Pandis, S. N.: 2010. Aged organic aerosol in the Eastern
553 Mediterranean: the Finokalia Aerosol Measurement Experiment – 2008.
554 *Atmos. Chem. Phys.*, 10, 4167–4186.
- 555 Hildemann, L. M., Cass, G. R., and Markowski, G. R.: A dilution stack sampler for
556 collection of organic aerosol emissions – design, characterization and field-
557 tests, *Aeros. Sci. Tech.*, 10, 193–204, 1989.
- 558 Huffman, J. A., Docherty, K. S., Aiken, A. C., Cubison, M. J., Ulbrich, I. M.,
559 DeCarlo, P. F., Sueper, D., Jayne, J. T., Worsnop, D. R., Ziemann, P. J., and
560 Jimenez, J. L.: Chemically-resolved aerosol volatility measurements from two
561 megacity field studies, *Atmos. Chem. Phys.*, 9, 7161–7182, 2009a.
- 562 Huffman, J. A., Docherty, K. S., Mohr, C., Cubison, M. J., Ulbrich, I. M., Ziemann,
563 P. J., Onasch, T. B., and Jimenez, J. L.: Chemically-resolved volatility
564 measurements of organic aerosol from different sources, *Environ. Sci.*
565 *Technol.*, 43, 5351–5357, 2009b.
- 566 Jayne, J. T., Leard, D. C., Zhang, X. F., Davidovits, P., Smith, K. A., Kolb, C. E., and
567 Worsnop, D. R.: Development of an aerosol mass spectrometer for size and
568 composition analysis of submicron particles, *Aerosol Sci. Tech.*, 33, 49–70,
569 2000.
- 570 Jimenez, J. L., Jayne, J. T., Shi, Q., Kolb, C. E., Worsnop, D. R., Yourshaw, I.,
571 Seinfeld, J. H., Flagan, R. C., Zhang, X., Smith, K. A., Morris, J., and



- 572 Davidovits, P.: Ambient aerosol sampling using the Aerodyne Aerosol Mass
573 Spectrometer, *J. Geophys. Res.*, 108, 8425, doi:10.1029/2001JD001213, 2003.
- 574 Jimenez, J. L., Canagaratna, M. R., Donahue, N. M., Prevot, A. S. H., Zhang, Q.,
575 Kroll, J. H., DeCarlo, P. F., Allan, J. D., Coe, H., Ng, N. L., Aiken, A. C.,
576 Docherty, K. D., Ulbrich, I. M., Grieshop, A. P., Robinson, A. L., Duplissy, J.,
577 Smith, J. D., Wilson, K. R., Lanz, V. A., Hueglin, C., Sun, Y. L., Tian, J.,
578 Laaksonen, A., T., R., Rautiainen, J., Vaattovaara, P., Ehn, M., Kulmala, M.,
579 Tomlinson, J. M., Collins, D. R., Cubison, M. J., Dunlea, E. J., Huffman, J.
580 A., Onasch, T. B., Alfarra, M. R., Williams, P. I., Bower, K., Kondo, Y.,
581 Schneider, J., Drewnick, F., Borrmann, S., Weimer, S., Demerjian, K.,
582 Salcedo, D., Cottrell, L., Griffin, R., Takami, A., Miyoshi, T., Hatakeyama, S.,
583 Shimono, A., Sun, J. Y., Zhang, Y. M., Dzepina, K., Kimmel, J. R., Sueper,
584 D., Jayne, J. T., Herndon, S. C., Trimborn, A. M., Williams, L. R., Wood, E.
585 C., Kolb, C. E., Baltensperger, U., and Worsnop, D. R.: Evolution of organic
586 aerosol in the atmosphere, *Science*, 326, 1525–1529, 2009.
- 587 Kanakidou, M., Seinfeld, J. H., Pandis, S. N., Barnes, I., Dentener, F. J., Facchini, M.
588 C., Van Dingenen, R., Ervens, B., Nenes, A., Nielsen, C. J., Swietlicki, E.,
589 Putaud, J. P., Balkanski, Y., Fuzzi, S., Horth, J., Moortgat, G. K.,
590 Winterhalter, R., Myhre, C. E. L., Tsigaridis, K., Vignati, E., Stephanou, E.
591 G., and Wilson, J.: Organic aerosol and global climate modelling: a review,
592 *Atmos. Chem. Phys.*, 5, 1053–1123, 2005.
- 593 Karydis, V. A., Tsimpidi, A. P., Fountoukis, C., Nenes, A., Zavala, M., Lei, W.,
594 Molina, L. T., and Pandis, S. N.: Simulating the fine and coarse inorganic
595 particulate matter concentrations in a polluted megacity, *Atmos. Environ.*, 44,
596 608–620, 2010.
- 597 Koo, B., Pandis, S. N., and Ansari, A.: Integrated approaches to modeling the organic
598 and inorganic atmospheric aerosol components, *Atmos. Environ.*, 37, 4757–
599 4768, 2003.
- 600 Kulmala, M., Asmi, A., Lappalainen, H. K., Carslaw, K. S., Pöschl, U.,
601 Baltensperger, U., Hov, Ø., Brenquier, J.-L., Pandis, S. N., Facchini, M. C.,
602 Hansson, H.-C., Wiedensohler, A., and O'Dowd, C. D.: Introduction:
603 European Integrated Project on Aerosol Cloud Climate and Air Quality
604 interactions (EUCAARI) - integrating aerosol research from nano to global
605 scales. *Atmos. Chem. Phys.*, 9, 2825–2841, 2009.
- 606 Lane, T. E., Donahue, N. M., and Pandis, S. N.: Simulating secondary organic aerosol
607 formation using the volatility basis-set approach in a chemical transport
608 model, *Atmos. Environ.*, 42, 7439–7451, 2008a.
- 609 Lane, T. E., Donahue, N. M., and Pandis, S. N.: Effect of NO_x on secondary organic
610 aerosol concentrations, *Environ. Sci. Technol.*, 42, 6022–6027, 2008b.
- 611 Lanz, V. A., Alfarra, M. R., Baltensperger, U., Buchmann, B., Hueglin, C., and
612 Prévôt, A. S. H.: Source apportionment of submicron organic aerosols at an
613 urban site by factor analytical modelling of aerosol mass spectra, *Atmos.*
614 *Chem. Phys.*, 7, 1503–1522, 2007.
- 615 Liang, C. K., Pankow J. F., Odum J. R., and Seinfeld J. H.: Gas/particle partitioning
616 of semi-volatile organic compounds to model inorganic, organic, and ambient
617 smog aerosols, *Environ Sci Technol*, 31, 3086-3092, 1997.
- 618 Lipsky, E. M. and Robinson, A. L.: Effects of dilution on fine particle mass and
619 partitioning of semivolatile organics in diesel exhaust and wood smoke.,
620 *Environ. Sci. Technol.*, 40, 155–162, 2006.



- 621 May, A. A., Levin, E. J. T., Hennigan, C. J., Riipinen, I., Lee, T., Collett, J. L.,
622 Jimenez, J. L., Kreidenweis, S. M., and Robinson, A. L.: Gas-particle
623 partitioning of primary organic aerosol emissions: 3. Biomass burning, *J.*
624 *Geophys. Res.*, 118, 11327–11338, 2013.
- 625 Morgan, W. T., Allan, J. D., Bower, K. N., Highwood, E. J., Liu, D., McMeeking, G.
626 R., Northway, M. J., Williams, P. I., Krejci, R., and Coe, H.: Airborne
627 measurements of the spatial distribution of aerosol chemical composition
628 across Europe and evolution of the organic fraction, *Atmos. Chem. Phys.*, 10,
629 4065–4083, 2010.
- 630 Morris, R. E., McNally, D. E., Tesche, T. W., Tonnesen, G., Boylan, J. W., and
631 Brewer, P.: Preliminary evaluation of the community multiscale air quality
632 model for 2002 over the southeastern united states, *J. Air Waste Manage.*, 55,
633 1694–1708, 2005.
- 634 Murphy, B. N. and Pandis, S. N.: Simulating the formation of semivolatile primary
635 and secondary organic aerosol in a regional chemical transport model,
636 *Environ. Sci. Technol.*, 43, 4722–4728, 2009.
- 637 Murphy, B. N., Donahue, N. M., Robinson, A. L., and Pandis, S. N.: A naming
638 convention for atmospheric organic aerosol, *Atmos. Chem. Phys.*, 14, 5825–
639 5839, 2014.
- 640 Ng, N. L., Kroll, J. H., Keywood, M. D., Bahreini, R., Varutbangkul, V., Flagan, R.
641 C., and Seinfeld, J. H.: Contribution of first- versus second-generation
642 products to secondary organic aerosols formed in the oxidation of biogenic
643 hydrocarbons, *Environ. Sci. Technol.*, 40, 2283–2297, 2006.
- 644 Ng, N. L., Canagaratna, M. R., Zhang, Q., Jimenez, J. L., Tian, J., Ulbrich, I. M.,
645 Kroll, J. H., Docherty, K. S., Chhabra, P. S., Bahreini, R., Murphy, S. M.,
646 Seinfeld, J. H., Hildebrandt, L., Donahue, N. M., DeCarlo, P. F., Lanz, V. A.,
647 Prévôt, A. S. H., Dinar, E., Rudich, Y., and Worsnop, D. R.: Organic aerosol
648 components observed in Northern Hemispheric datasets from Aerosol Mass
649 Spectrometry, *Atmos. Chem. Phys.*, 10, 4625–4641, 2010.
- 650 O’Dowd, C. D., Langmann, B., Varghese, S., Scannell, C., Ceburnis, D., and
651 Facchini, M. C.: A Combined Organic-Inorganic Sea-Spray Source Function,
652 *Geophys. Res. Lett.*, 35, L01801, doi:10.1029/2007GL030331, 2008.
- 653 Odum, J. R., Hoffman, T., Bowman, F., Collins, D., Flagan, R. C., and Seinfeld, J. H.:
654 Gas/particle partitioning and secondary organic aerosol yields, *Environ. Sci.*
655 *Technol.*, 30, 2580–2585, 1996.
- 656 Paatero, P. and Tapper, U.: Positive matrix factorization – a nonnegative factor
657 model with optimal utilization of error-estimates of data values,
658 *Environmetrics*, 5, 111–126, 1994.
- 659 Pankow, J. F.: Review and comparative-analysis of the theories on partitioning
660 between the gas and aerosol particulate phases in the atmosphere, *Atmos.*
661 *Environ.*, 21, 2275–2283, 1987.
- 662 Pankow, J. F.: An absorption-model of gas-particle partitioning of organic-
663 compounds in the atmosphere, *Atmos. Environ.*, 28, 185–188, 1994.
- 664 Presto, A. A. and Donahue, N. M.: Investigation of α -pinene + ozone secondary
665 organic aerosol formation at low total aerosol mass, *Environ. Sci. Technol.*,
666 40, 3536–3543, 2006.
- 667 Pope, C. A.: Respiratory hospital admission associated with PM₁₀ pollution in Utah,
668 Salt Lake and Cache Valleys, *Archives of Environmental Health*. 7, 46–90,
669 1991.



- 670 Puxbaum, H., Caseiro, A., Sanchez-Ochoa, A., Kasper-Giebl, A., Claeys, M.,
671 Gelencser, A., Legrand, M., Preunkert, S., and Pio, C.: Levoglucosan levels at
672 background sites in Europe for assessing the impact of biomass combustion on
673 the aerosol European background, *J. Geophys. Res.* 112, D23S05,
674 doi:10.1029/2006JD008114, 2007.
- 675 Roberts, G. C., Andreae, M. O., Zhou, J., and Artaxo, P.: Cloud condensation nuclei
676 in the Amazon Basin: “Marine” conditions over a continent?, *Geophys. Res.*
677 *Lett.*, 28, 2807–2810, 2001.
- 678 Robinson, A. L., Donahue, N. M., Shrivastava, M. K., Weitkamp, E. A., Sage, A. M.,
679 Grieshop, A. P., Lane, T. E., Pierce, J. R., and Pandis, S. N.: Rethinking
680 organic aerosol: semivolatile emissions and photochemical aging, *Science*,
681 315, 1259–1262, 2007.
- 682 Roth, C. M., Goss K. U., and Schwarzenbach R. P.: Sorption of a diverse set of
683 organic vapors to diesel soot and road tunnel aerosols, *Environ Sci Technol*,
684 39, 6632–6637, 2005.
- 685 Schwartz, J., Dockery D. W., and Neas L. M.: Is daily mortality associated
686 specifically with fine particles?, *J. Air Waste Manag. Assoc.*, 46, 927–939,
687 1996.
- 688 Seinfeld, J. H. and Pandis, S. N.: *Atmospheric Chemistry and Physics: From Air*
689 *Pollution to Global Change*, second ed. J. Wiley and Sons, New York, 2006.
- 690 Shrivastava, M. K., Lipsky, E. M., Stanier, C. O., and Robinson, A. L.: Modeling
691 semivolatile organic aerosol mass emissions from combustion systems.
692 *Environ. Sci. Technol.*, 40, 2671–2677, 2006.
- 693 Shrivastava, M. K., Lane, T. E., Donahue, N. M., Pandis, S.N., and Robinson, A. L.:
694 Effects of gas-particle partitioning and aging of primary emissions on urban
695 and regional organic aerosol concentrations, *J. Geophys. Res.*, 113, D18301,
696 doi:10.1029/2007JD009735, 2008.
- 697 Skamarock, W. C., Klemp, J. B., Dudhia, J., Gill, D. O., Barker, D. M., Wang, W.,
698 and Powers, J. G.: A Description of the Advanced Research WRF Version 2.
699 NCAR Technical Note (<http://www.mmm.ucar.edu/wrf/users/docs/arwv2.pdf>),
700 2005.
- 701 Sofiev, M., Vankevich, R., Lanne, M., Koskinen, J., and Kukkonen, J.: On integration
702 of a Fire Assimilation System and a chemical transport model for near-real-
703 time monitoring of the impact of wild-land fires on atmospheric composition
704 and air quality, *Modelling, Monitoring and Management of Forest Fires*, *Wit*
705 *Trans. Ecol. Envir.*, 119, 343–351, 2008a.
- 706 Sofiev, M., Lanne, M., Vankevich, R., Prank, M., Karppinen, A., and Kukkonen, J.:
707 Impact of wild-land fires on European air quality in 2006–2008, *Modelling,*
708 *Monitoring and Management of Forest Fires*, *Wit Trans. Ecol. Envir.*, 119,
709 353–361, 2008b.
- 710 Stanier, C. O., Donahue, N. M., and Pandis, S. N.: Parameterization of secondary
711 organic aerosol mass fraction from smog chamber data, *Atmos. Environ.*, 42,
712 2276–2299, 2008.
- 713 Takegawa, N., Miyazaki, Y., Kondo, Y., Komazaki, Y., Miyakawa, T., Jimenez, J. L.,
714 Jayne, J. T., Worsnop, D. R., Allan, J., and Weber, R. J.: Characterization of
715 an Aerodyne Aerosol Mass Spectrometer (AMS): Intercomparison with other
716 aerosol instruments, *Aeros. Sci. Tech.*, 39, 760–770, 2005.
- 717 Tsimpidi, A. P., Karydis, V. A., Zavala, M., Lei, W., Molina, L., Ulbrich, I. M.,
718 Jimenez, J. L., and Pandis, S. N.: Evaluation of the volatility basis-set



- 719 approach for the simulation of organic aerosol formation in the Mexico City
720 metropolitan area, *Atmos. Chem. Phys.*, 10, 525–546, 2010.
- 721 Ulbrich, I. M., Canagaratna, M. R., Zhang, Q., Worsnop, D. R., and Jimenez, J. L.:
722 Interpretation of organic components from Positive Matrix Factorization of
723 aerosol mass spectrometric data, *Atmos. Chem. Phys.*, 9, 2891–2918, 2009.
- 724 Visschedijk, A. J. H., Zandveld, P., and Denier van der Gon, H. A. C.: TNO Report
725 2007 A-R0233/B: A high resolution gridded European emission database for
726 the EU integrated project GEMS, The Netherlands, Organization for Applied
727 Scientific Research, 2007.
- 728 Wang, Z., Hopke P. K., Ahmadi G., Cheng Y. S., and Baron P. A.: Fibrous particle
729 deposition in human nasal passage: The influence of particle length, flow rate,
730 and geometry of nasal airway, *J. Aerosol Sci.*, 39, 1040–1054, 2008.
- 731 Zhang, Q., Canagaratna, M. C., Jayne, J. T., Worsnop, D. R., and Jimenez, J. L.: Time
732 and size-resolved chemical composition of submicron particles in Pittsburgh
733 Implications for aerosol sources and processes, *J. Geophys. Res.*, 110,
734 D07S09, doi:10.1029/2004JD004649, 2005.
- 735 Zhang, Q., Jimenez, J. L., Canagaratna, M. R., Allan, J. D., Coe, H., Ulbrich, I.,
736 Alfarra, M. R., Takami, A., Middlebrook, A. M., Sun, Y. L., Dzepina, K.,
737 Dunlea, E., Docherty, K., De-Carlo, P., Salcedo, D., Onasch, T. B., Jayne, J.
738 T., Miyoshi, T., Shimono, A., Hatakeyama, N., Takegawa, N., Kondo, Y.,
739 Schneider, J., Drewnick, F., Weimer, S., Demerjian, K. L., Williams, P. I.,
740 Bower, K. N., Bahreini, R., Cottrell, L., Griffin, R. J., Rautianen, J., and
741 Worsnop, D. R.: Ubiquity and dominance of oxygenated species in organic
742 aerosols in anthropogenically-influenced Northern Hemisphere midlatitudes.
743 *Geophys. Res. Lett.*, 34, L13801, doi:10.1029/2007GL029979, 2007.

1 **Table 1.** Parameters used to simulate POA and bbPOA emissions in PMCAMx-SR.

2

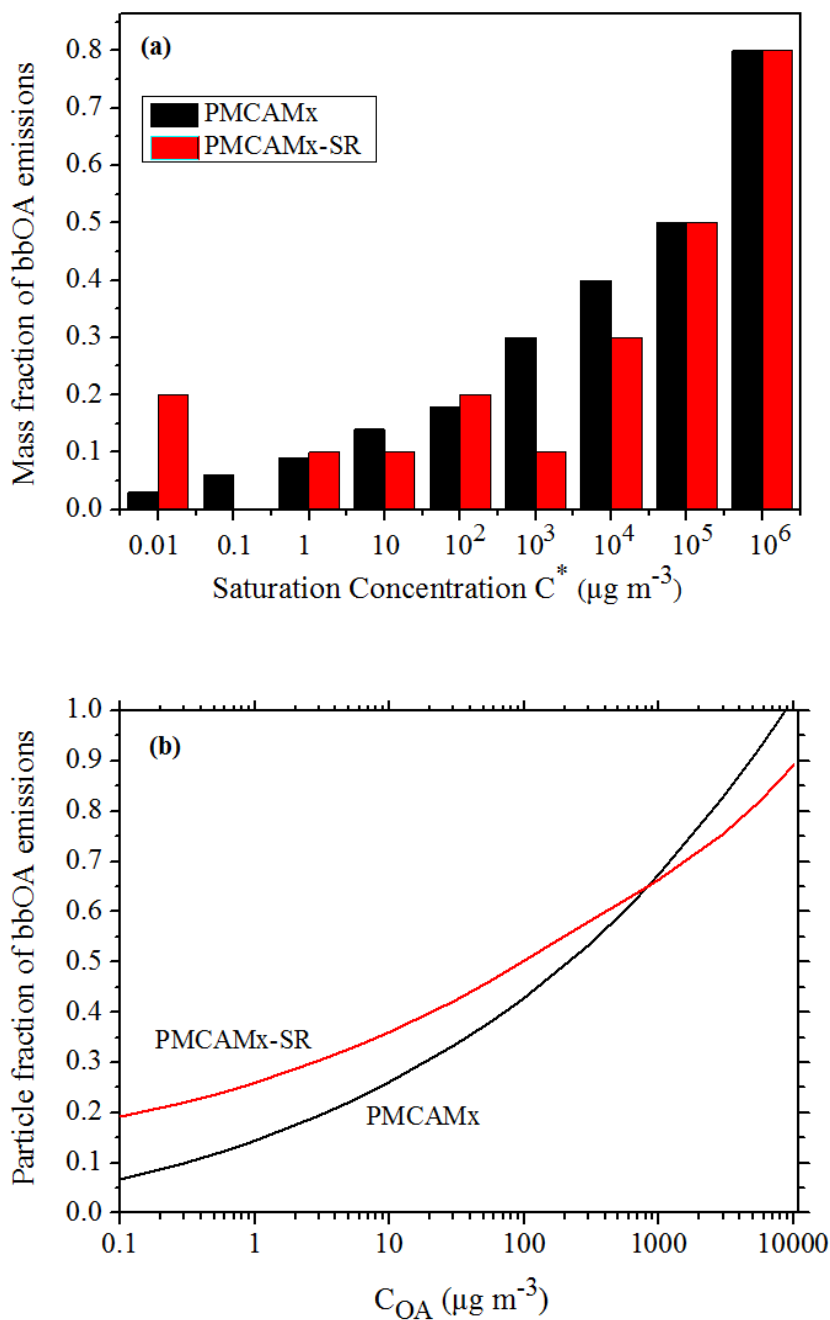
C^* at 298 K ($\mu\text{g m}^{-3}$)	10^{-2}	10^{-1}	10^0	10^1	10^2	10^3	10^4	10^5	10^6
POA									
Fraction of POA emissions ¹	0.03	0.06	0.09	0.14	0.18	0.30	0.40	0.50	0.80
Effective Vaporization Enthalpy (kJ mol^{-1})	112	106	100	94	88	82	76	70	64
bbPOA (Base Case)									
Fraction of POA emissions	0.2	0.0	0.1	0.1	0.2	0.1	0.3	0.50	0.80
Effective Vaporization Enthalpy (kJ mol^{-1})	93	89	85	81	77	73	69	70	64
bbPOA (Sensitivity Test)									
Fraction of POA emissions	0.2	0.0	0.1	0.1	0.2	0.1	0.3	-	-
Effective Vaporization Enthalpy (kJ mol^{-1})	93	89	85	81	77	73	69	-	-

¹This is the traditional non-volatile POA included in inventories used for regulatory purposes. The sum of all fractions can exceed unity because a large fraction of the IVOCs is not included in these traditional particle emission inventories.



- 1 **Table 2.** Organic compound emission rates (in tn d^{-1}) over the modeling domain
- 2 during the simulated periods.

Emission rate (tn d^{-1})	
1 – 29 May 2008	
Wildfires	1,700
Residential	700
Agriculture - waste burning	300
25 February – 22 March 2009	
Wildfires	3,000
Residential	6,000
Agriculture - waste burning	320



1

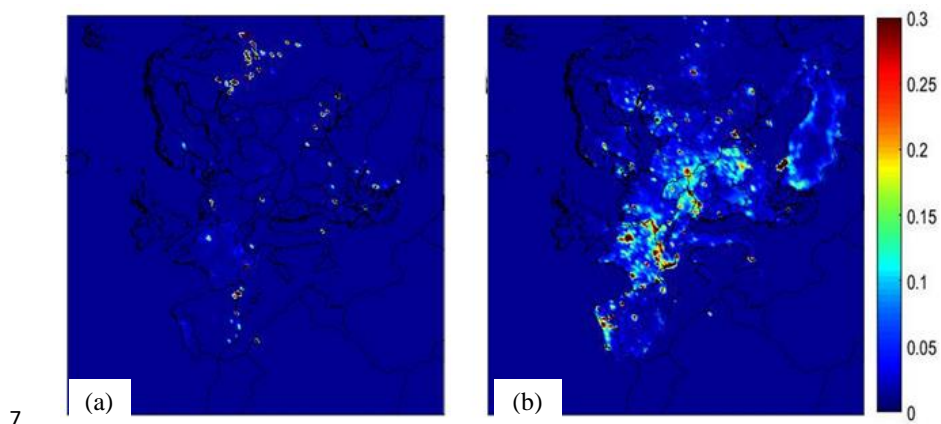
2

3

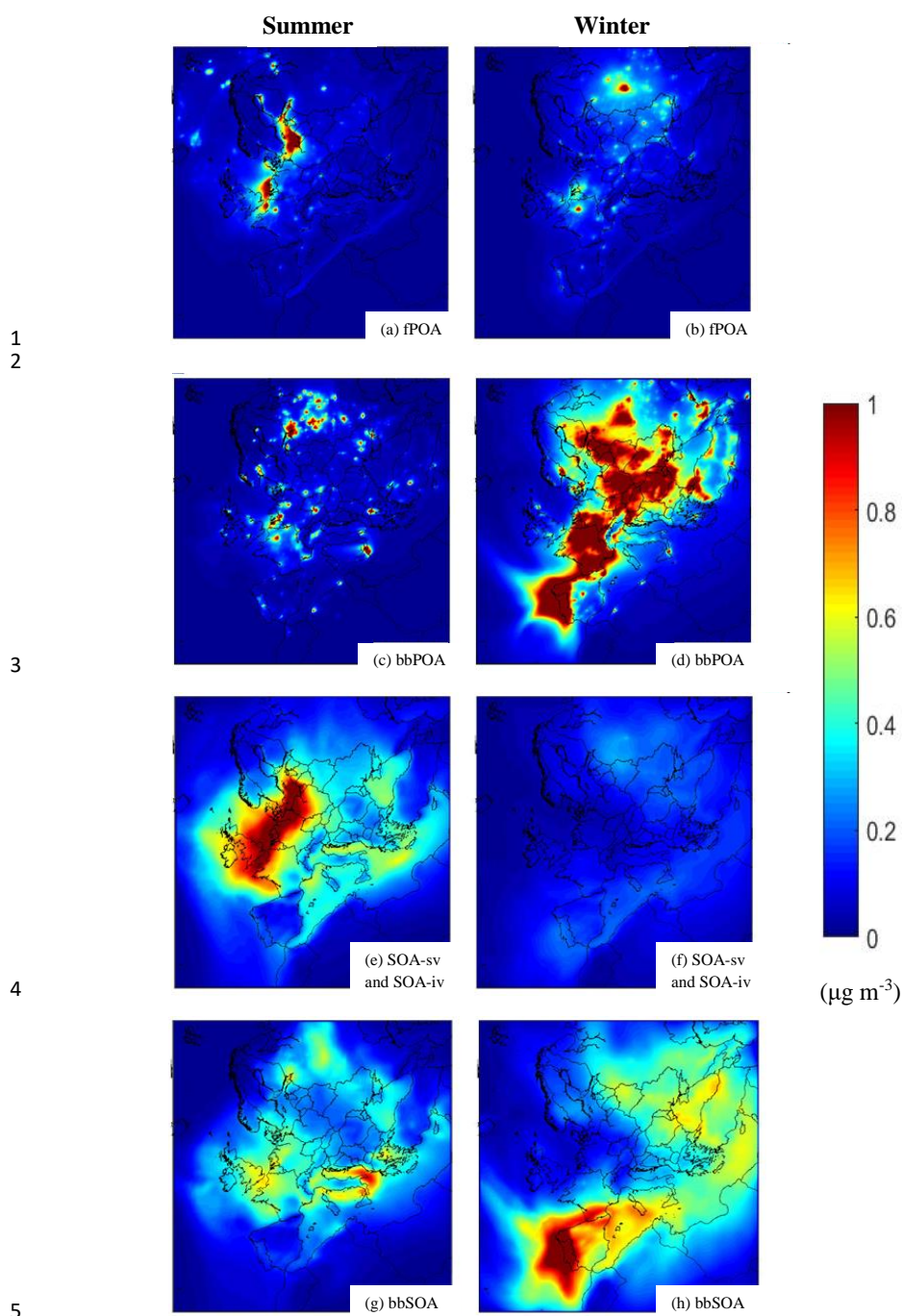
4 **Figure 1.** (a) Volatility distribution of bbOA in PMCAMx and PMCAMx-SR. (b)

5 Particle fractions of bbOA emissions as a function of OA concentration at 298 K.

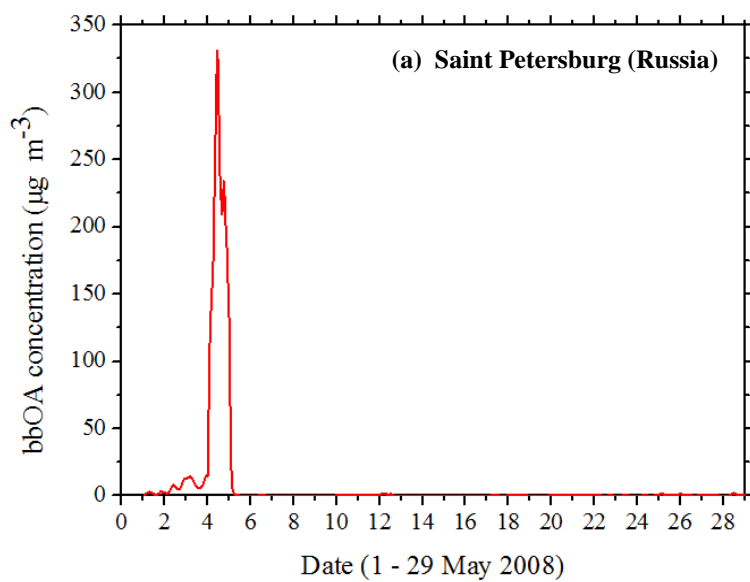
6



9 **Figure 2.** Spatial distribution of average biomass burning OA emission rates (kg d^{-1}
10 km^{-2}) for the two simulation periods: (a) 1-29 May 2008 and (b) 25 February-22
11 March 2009.

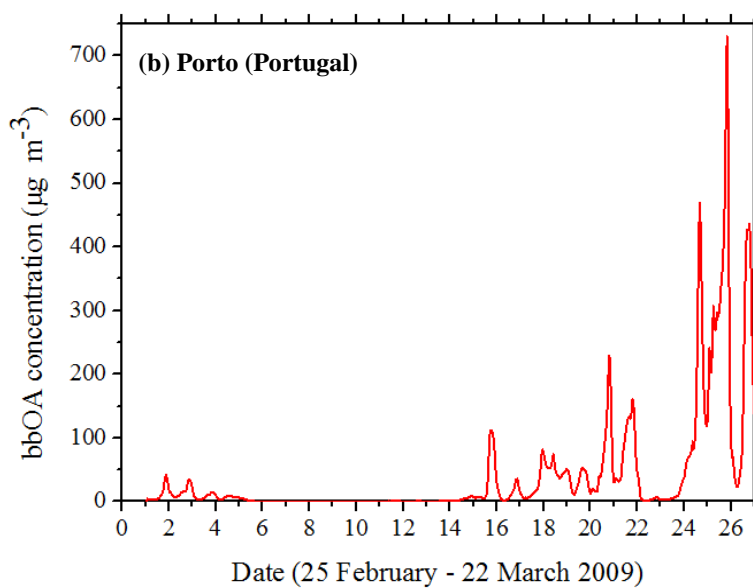


6 **Figure 3.** PMCAMx-SR predicted base case ground – level concentrations of PM_{2.5}
 7 (a-b) fPOA, (c-d) bbPOA, (e-f) SOA and (g-h) bbSOA, during the modeled summer
 8 and winter periods.



1

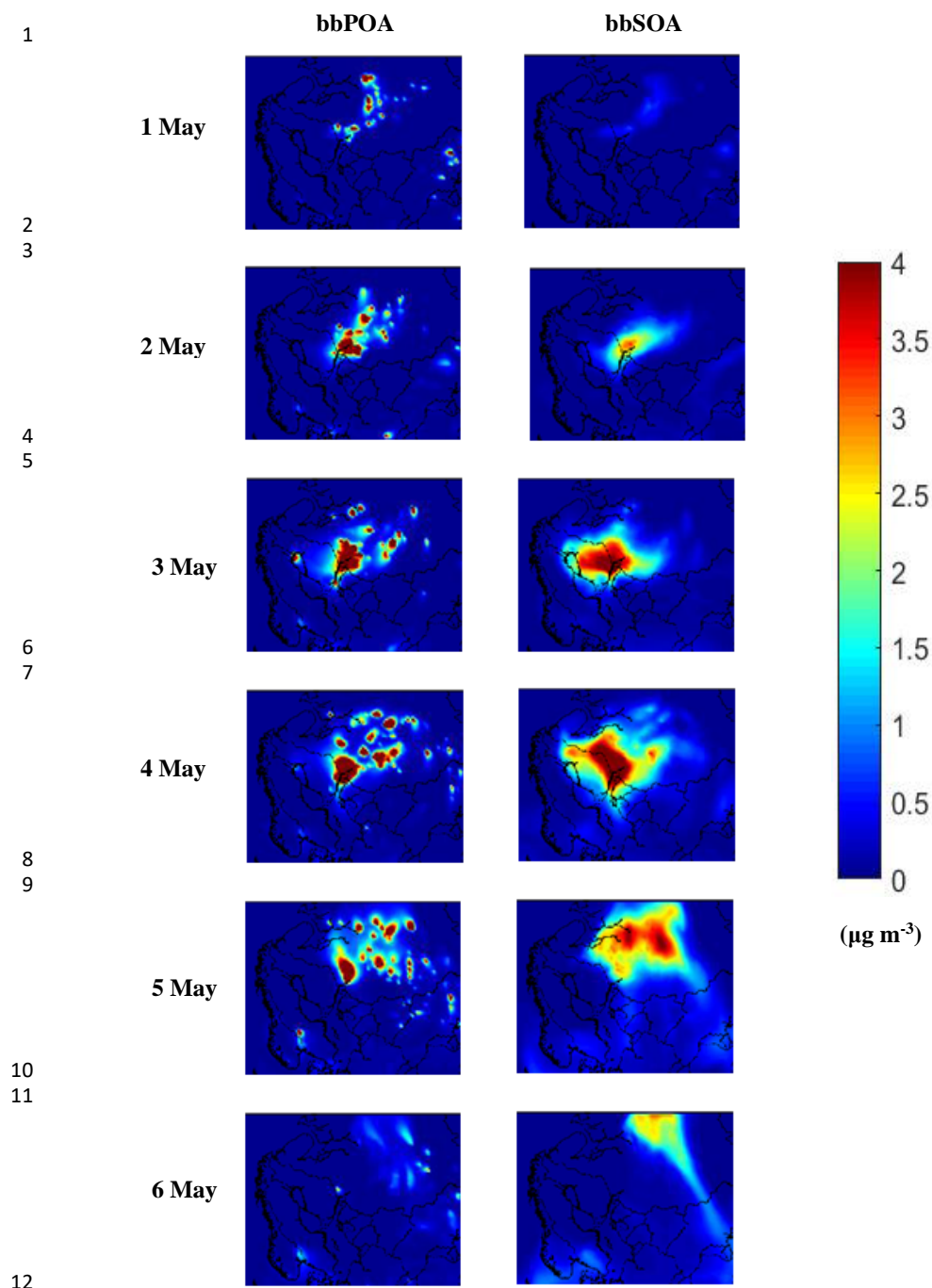
2



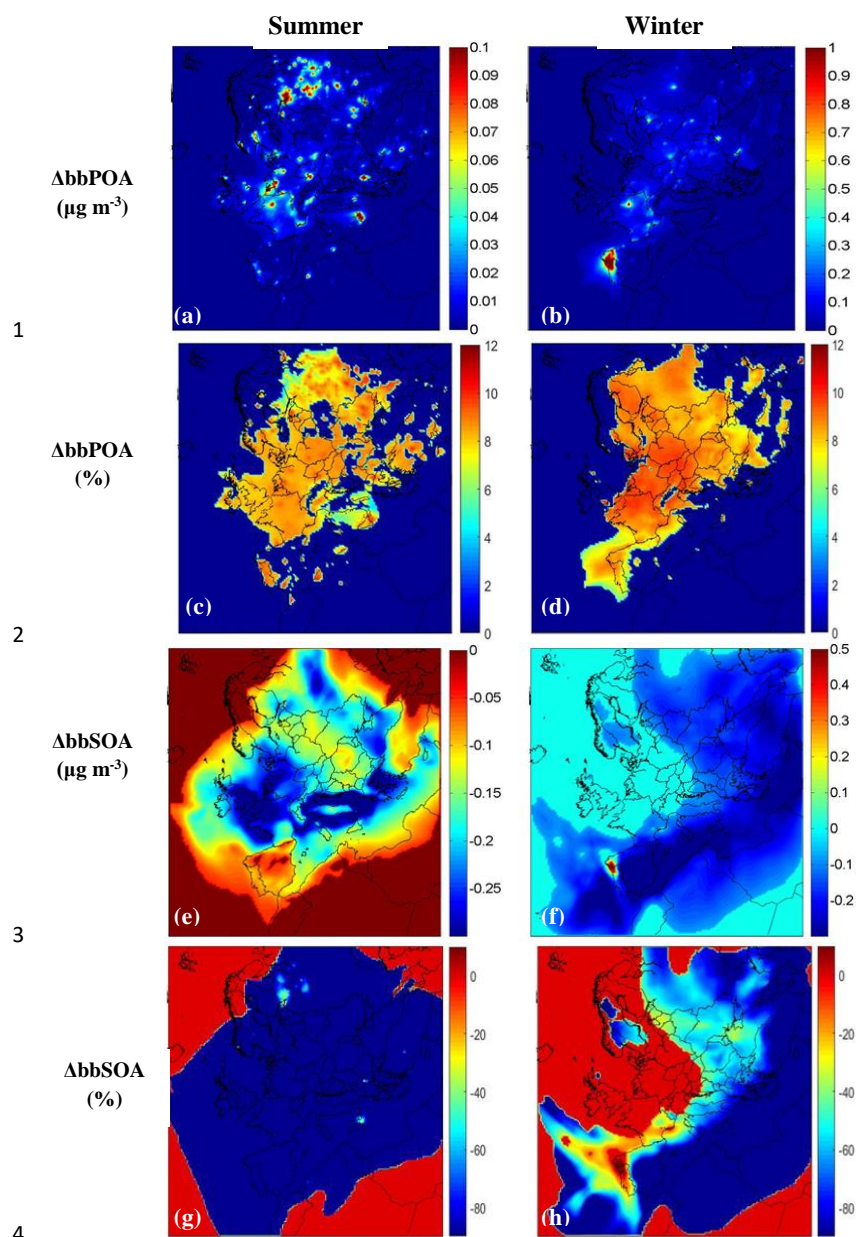
3

4 **Figure 4.** Timeseries of PM_{2.5} bbOA concentrations in (a) Saint Petersburg in Russia
5 during 1-29 May 2008 and in (b) Porto in Portugal during 25 February-22 March
6 2009.

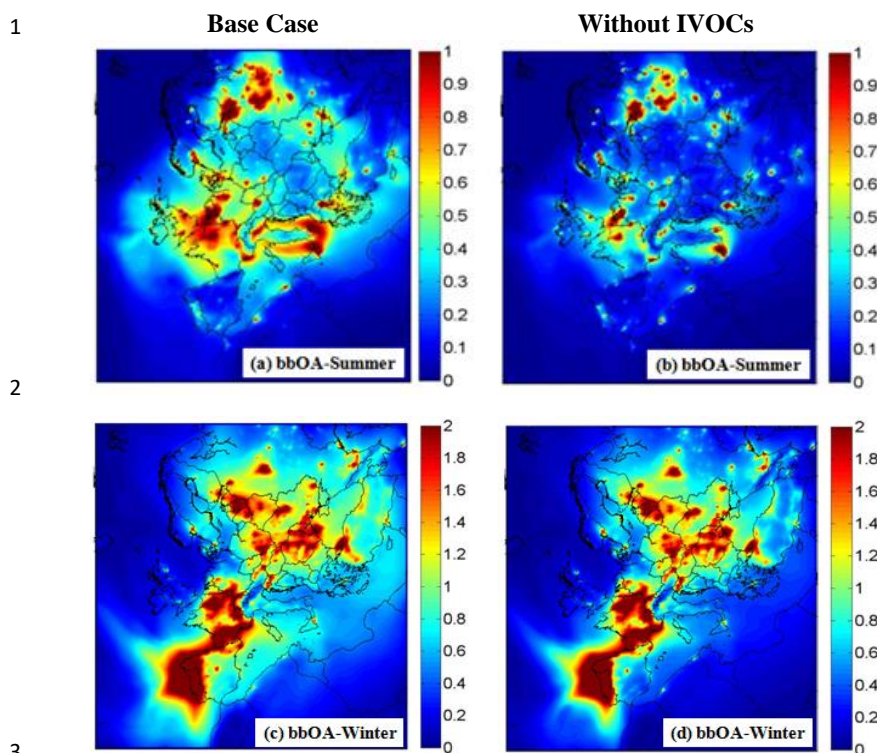
7



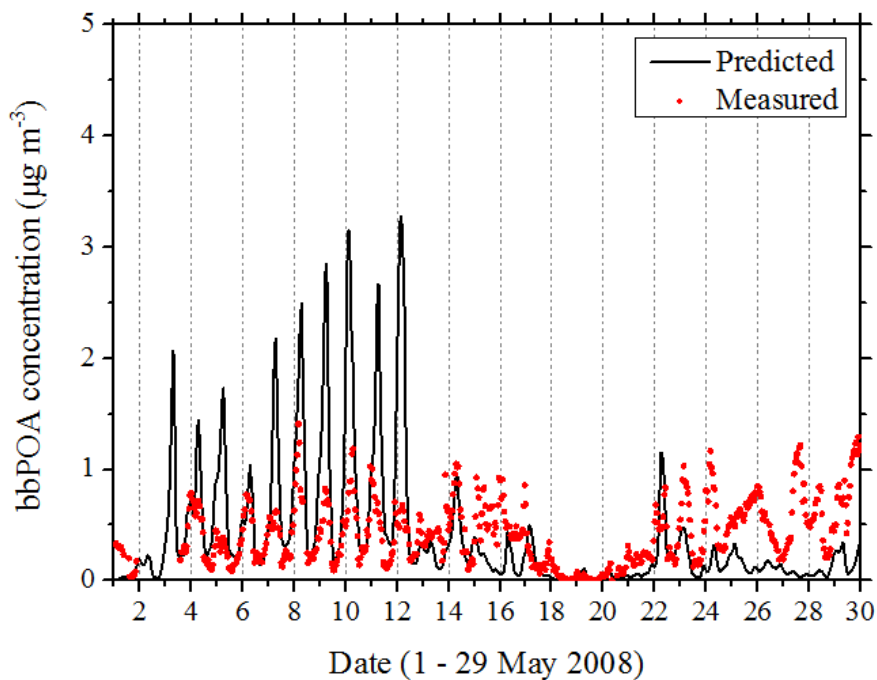
13 **Figure 5.** PMCAMx-SR predicted base case ground – level concentrations of $PM_{2.5}$
 14 bbPOA and bbSOA, during 1 – 6 May 2008 in the Scandinavian Peninsula and
 15 Russia.



5 **Figure 6.** Average predicted absolute ($\mu\text{g m}^{-3}$) difference (Sensitivity Case – Base
6 Case) of ground-level $\text{PM}_{2.5}$ (a-b) bbPOA and (e-f) bbSOA concentrations from
7 PMCAMx-SR base case and sensitivity simulations during the modeled periods. Also
8 shown the corresponding relative (%) change of ground-level $\text{PM}_{2.5}$ (c-d) bbPOA and
9 (g-h) bbSOA concentrations during the modeled periods. Positive values indicate that
10 PMCAMx-SR sensitivity run predicts higher concentrations.



5 **Figure 7.** Predicted ground-level concentrations of PM_{2.5} total bbOA ($\mu\text{g m}^{-3}$) during
6 the modeled summer (a-b) and the modeled winter (c-d) period. The figures to the left
7 are for the PMCAMx-SR base case simulation while those to the right for the low-
8 IVOC sensitivity test.



1

2 **Figure 8.** Comparison of hourly bbPOA concentrations predicted by PMCAMx-SR
3 with values estimated by PMF analysis of the AMS data in Cabauw during 1-29 May
4 2008.